Application Note

Cell Migration and Invasion

Agilent

Trusted Answers

Incorporation of a Novel, Automated Scratch Tool and Kinetic Label-Free Imaging to Perform Wound Healing Assays

Author

Brad Larson
Agilent Technologies, Inc.

Abstract

The wound healing or "scratch" assay is one of the most highly used *in vitro* methods to monitor and quantify collective cell migration. The current standard involves manual wound creation, which yields low reproducibility between wounds, high variability within generated data, and possible false conclusions regarding test molecules. Using an automated wound creation tool, in addition to kinetic image capture and analysis, repeatable wounds and robust and repeatable results are easily attained.

Introduction

The movement of cells when influenced by interactions with neighboring cells, otherwise known as collective cell migration, plays a role in numerous critical physiological processes, including morphogenesis and tissue regeneration.[1] This type of movement as a cohesive group has also been shown to be critical in wound healing and cancer metastasis. In wound healing, epithelial cells collectively migrate as a sheet of cells. Wounding of the epithelial layer induces cell migration in a directional manner. During this process, cells maintain tight intercellular adhesion, healing the original wound.[2] Similarly, collective cell migration has also been implicated as playing a major role in cancer metastasis. An increasing number of publications indicate that metastatic cells cluster and invade collectively in the vasculature and lymphatics of cancer patients.[3-4] Therefore, attaining a better understanding of collective cell movement is of critical value for the treatment of multiple disease types.

One of the most widely used methods to measure collective cell migration is the wound healing or "scratch" assay. Following creation of a wound, or cell-free zone, within the confluent cell layer, cell movement back into the wound area is monitored over time using cellular imaging. Kinetic and endpoint data then allow for quantification of cell migration, either when uninhibited or under the influence of a test molecule. For wound creation, commonly a pipette tip is manually dragged through the cells, which can lead to wounds that vary drastically in width, orientation, and in placement within the well. This yields increased variability in calculated measurements within replicate wells and across titrations, complicating final conclusions regarding the migratory ability of test cell models and treatments, especially when comparing assay to assay data. To increase the robustness of generated data, a method to create consistent wounds is necessary.

This study demonstrates the use of a novel, automated tool to create scratch wounds in cell monolayers formed on the bottom of a microplate. With the single push of a button, and using a 4- or 8-pin head, consistent scratches of equivalent size and area are made in either 24- or 96-well plates. A multi-reservoir cleaning trough is also incorporated on the deck of the tool. Using the onboard programmed procedure, unattended cleaning and decontamination of each pin is accomplished before and after use. The small footprint permits insertion of the tool; using any size laminar flow hood enabling wound creation in a sterile manner. Following washing, the plate can then be transferred to an Agilent BioTek automated imager or the Agilent BioTek BioSpa live cell analysis system to kinetically monitor cell migration.

Materials and methods

Materials

Cells

HT-1080 fibrosarcoma cells (part number CCL-121) were purchased from ATCC (Manassas, VA). Human neonatal dermal fibroblasts expressing RFP (part number cAP-0008RFP) were purchased from Angio-Proteomie (Boston, MA). U-87 glioblastoma cells expressing GFP were generously donated by Dr. Sachin Katyal (University of Manitoba, Winnipeg, Manitoba, Canada).

Experimental components

Advanced DMEM (part number 12491- 015), fetal bovine serum (part number 10437-036), penicillin-streptomycin-glutamine (100x) (part number 10378-016), TrypLE express enzyme (1x), phenol red (part number 12605-010), Alconox powdered precision cleaner (part number 16-000-104), Virkon-S (part number NC9821357), and CellTracker Green CMFDA Dye (part number C2925) were purchased from Thermo Fisher Scientific (Waltham, MA). Cytochalasin D (part number 1233) was purchased from Bio-Techne Corporation (Minneapolis, MN). 24-well clear TC-treated multiple well plates (part number 3524) and 96-well clear, flat bottom, polystyrene TC-treated microplates (part number 3598) were purchased from Corning Life Sciences (Corning, NY).

Agilent BioTek AutoScratch wound making tool

The Agilent BioTek AutoScratch wound making tool automatically creates reproducible scratch wounds in cell monolayers grown in microplates. The simple pushbutton operation and tool-free scratch pin manifold exchange make it easy to process either 96- or 24-well plates, which are commonly used in migration and invasion assays. The compact system features an onboard, preprogrammed cleaning routine to keep the scratch pins free of buildup and avoiding contamination. AutoScratch precisely and efficiently automates the sample prep for imaging workflows with Agilent BioTek Cytation cell imaging multimode readers and Agilent BioTek Lionheart automated microscopes.

Agilent BioTek Cytation 5 cell imaging multimode reader

Cytation 5 is a modular multimode microplate reader combined with an automated digital microscope. Filter- and monochromator-based microplate reading are available, and the microscopy module provides up to 60x magnification in fluorescence, brightfield, color brightfield and phase contrast. The instrument can perform fluorescence imaging in up to four channels in a single step. With special emphasis on live cell assays, Cytation 5 features shaking, temperature control to 65 °C, CO_2/O_2 gas control and dual injectors for kinetic assays and is controlled by integrated Agilent BioTek Gen5 microplate reader and imager software, which also automates image capture, analysis and processing. The instrument was used to capture kinetic high contrast brightfield and fluorescent images over the incubation period.

Agilent BioTek BioSpa 8 automated incubator

The BioSpa 8 automated incubator links Agilent BioTek readers or imagers together with Agilent BioTek washers and dispensers for full workflow automation of up to eight microplates. Temperature, CO_2/O_2 and humidity levels are controlled and monitored through the Agilent BioTek BioSpa software to maintain an ideal environment for cell cultures during all experimental stages. Test plates were incubated in the BioSpa to maintain proper atmospheric conditions during incubation and automatically transferred to the Cytation 5 for high contrast brightfield and fluorescent imaging.

Agilent BioTek MultiFlo FX multimode dispenser

The MultiFlo FX is a modular, upgradable reagent dispenser that can have as many as two peristaltic pump (8-tube dispensers), two syringe pump dispensers and a strip washer. The syringe and washer manifolds can be configured for plate densities from 6- to 384-well.

Methods

Cell preparation

Cells were cultured in T-75 flasks until reaching 80% confluency. Subsequent to detachment from the flask with TrypLE, cells were resuspended to preoptimized concentrations depending on plate well density and culture conditions (Table 1).

Table 1. Automated 3D tumoroid invasion imaging parameters.

Cell Plating Concentrations		
	24-Well Format	**96-Well Format**
HT-1080	2.4×10^5 cells/mL	4.0×10^5 cells/mL
Fibroblast	–	2.0×10^5 cells/mL
U-87	2.4×10^5 cells/mL	4.0×10^5 cells/mL

AutoScratch cleaning procedure

Prior to wound creation in test plates, the AutoScratch tool pins were cleaned and sterilized. The four cleaning components were added to individual reservoirs of the cleaning trough, labeled to assist with appropriate component and volume addition (Table 2).

Table 2. Cleaning trough reagent setup.

AutoScratch Cleaning Components		
Reservoir 1	Alconox, 0.5%	12 mL
Reservoir 2	Virkon-S, 1%	12 mL
Reservoir 3	Sterile DI H_2O	12 mL
Reservoir 4	70% Ethanol	12 mL

The “Clean” button was pressed to initiate the cleaning procedure. During the process, the scratching arm containing the pins moves from the home position into the reservoir containing 0.5% Alconox, agitates in the Y-axis for 3 seconds, then soaks the pins in the component for 5 minutes. At the completion of the 5-minute incubation period, the arm moves the pins to the Virkon-S. The process is then automatically repeated for each of the remaining components. At the end of the 20-minute cleaning cycle, the pins were cleaned, sterilized, and ready to be used for wound creation.

Scratch wound creation

Following completion of the cleaning procedure, the test plate was added to the deck of the AutoScratch tool and the lid removed. The “Scratch” button appropriate for the microplate density being used, “24” or “96”, was pressed to begin the wounding process. Here the arm moves the pins from the home position to column 1 of the plate where a scratch is made vertically at the center of the well. The arm then moves the pins back to the reservoir containing the DI H_2O and performs a three second agitation to remove any dislodged cells sticking to the pins. The pins are then moved to column 2 and the scratching and cleaning steps are repeated for each column of the plate.

Post scratch plate washing

Upon completion of the wound creation routine, the plate was transferred to a separate laminar flow hood containing the Agilent BioTek MultiFlo FX. Here a plate washing procedure was carried out to remove cells dislodged from the bottom of the plate. The stainless steel tubes of the strip washer, previously sterilized using 70% ethanol, were used to aspirate media while the peristaltic pump and an autoclaved 5 uL cassette dispensed back fresh media. For uninhibited wells, the procedure was repeated 3x. For wells containing the cytochalasin D titration, media containing inhibitor was added manually following the third aspiration cycle.

Kinetic image-based monitoring of cell migration

Plates were then placed into the BioSpa 8, with atmospheric conditions previously set to 37 °C/5% CO_2. Water was added to the pan to create a humidified environment. The BioSpa 8 software was programmed such that the plates were automatically transferred to Cytation 5 for high contrast brightfield or high contrast brightfield and fluorescent imaging of the test wells, depending on the incorporated cell types. A single 4x image was taken with each channel (Table 3) to capture potential cell movement into the original wound area.

Table 3. Included imaging channels per test cell model.

Incorporated Imaging Channels	
HT-1080	High contrast brightfield/GFP
Fibroblast	High contrast brightfield/RFP
U-87	High contrast brightfield/GFP

Plates were then transferred back to the BioSpa 8. Kinetic imaging cycles were carried out using iterations optimized depending on the speed of migration for each cell model (Table 4).

Table 4. Optimized imaging intervals per cell model.

Kinetic Imaging Intervals	
HT-1080	60 minutes
Fibroblast	90 minutes
U-87	90 minutes
Fibroblast/U-87 Co-culture	90 minutes

Image processing

Following capture, using the settings in Table 5, high contrast brightfield images were processed to increase the contrast in brightfield signal between background and cell containing areas of the image, while fluorescent images were processed to remove background signal.

Table 5. Image preprocessing parameters.

Incorporated Imaging Channels				
Channel	Apply Image Processing	Background	Rolling Ball	Priority
High Contrast Brightfield	Yes	Dark	25 µm	Fine results
RFP	Yes	Dark	Auto	Fine results
GFP	Yes	Dark	Auto	Fine results

Cellular analysis of preprocessed images

Cellular analysis was carried out on the processed images to quantify the cell containing areas of each image using the criteria in Table 6.

Table 6. Object mask analysis parameters.

Primary Cellular Analysis Parameters	
Channel	Tsf[Brightfield]
Threshold	2,000
Background	Dark
Split Touching Objects	Unchecked
Fill Holes in Masks	Checked
Minimum Object Size	100 µm
Maximum Object Size	10,000 µm
Include Primary Edge Objects	Checked
Analyze Entire Image	Checked
Advanced Detection Options	
Rolling Ball Diameter	40
Image Smoothing Strength	20
Evaluate Background On	1% of lowest pixels
Expand the Threshold Mask	5 µm
Analysis Metric	
Metric of Interest	Object sum area

Wound healing metric calculation

The kinetic cell area coverage values (object sum area) were then used to generate three additional wound healing metrics, including wound width, wound confluence, and maximum wound healing rate. Each metric is automatically calculated by the Agilent BioTek Gen5 wound healing protocol.

Wound width

Wound width, or the average width of the cell-free zone over time, is calculated using the following formula:

$$\frac{W_t = I_A - \text{Object Sum Area}_t}{I_H}$$

Where W_t is the average wound width (µm) over time, I_A is the total area of the 4x image, Object Sum Area_t is the area covered by cells at each time point, and I_H is the height of a 4x image.

Wound confluence

Wound confluence, or the percentage of the original wound area covered by migrating cells over time, is calculated using the following formula:

$$C_t = \frac{\text{Object Sum Area}_t - \text{Object Sum Area}_0 * 100}{I_A - \text{Object Sum Area}_0}$$

Where C_t is the percent wound confluence over time, Object Sum Area$_t$ is the area covered by cells at each time point, Object Sum Area$_0$ is the area covered by cells at time 0, and I_A is the total area of the 4x image.

Maximum wound healing rate

The maximum wound healing rate is calculated using a Kinetic Analysis step in Gen5. The Max V calculation type is selected and the rate is calculated using six data points along the sum area curve. The value is then expressed as μm^2 per hour.

Results and discussion

Validation of consistency within scratch wound creation

To validate the ability of the Agilent BioTek AutoScratch unit to create wounds of a consistent size, HT-1080 cells were plated into each well of 96-well microplates using a volume of 100 µL and a concentration of 4.0×10^5 cells/mL. Following an overnight incubation to allow for attachment, the plates were placed one at a time onto the deck and scratched by the AutoScratch tool to create wounds in each well. Visual inspection of the high contrast brightfield images illustrated the consistent wound shape and size that could be achieved from well to well (Figure 1).

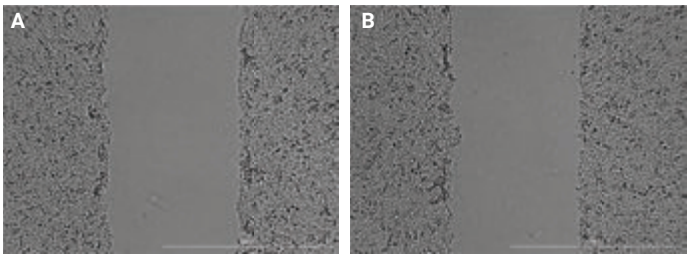

Figure 1. Images captured from a 96-well plate immediately following wound creation with the Agilent BioTek AutoScratch using the high contrast brightfield imaging channel and a 4x objective.

Validation of consistent wound creation was also performed in 24-well plates. Here HT-1080 cells were added to each well using a volume of 1 mL and concentration of 2.4×10^5 cells/mL. Following the overnight cell attachment incubation period, the plates were again placed onto the deck and scratched by the Agilent BioTek AutoScratch tool. Visual inspection of high contrast brightfield images captured from the 24-well plate once again illustrated consistent wound shape and size similar to that seen from the 96-well plates (Figure 2).

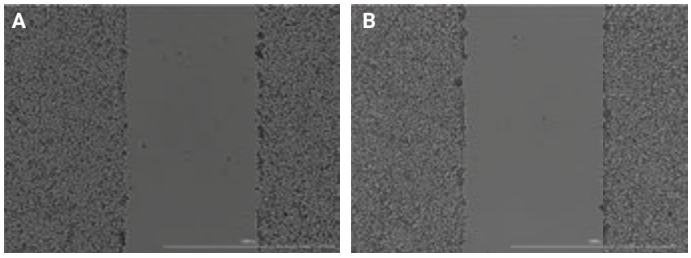

Figure 2. Images captured from a 24-well plate immediately following wound creation with the Agilent BioTek AutoScratch using the high contrast brightfield imaging channel and a 4x objective.

To quantify the consistency of wound creation, high contrast brightfield images (Figure 3A) were then preprocessed using the parameters described in Table 5. Using this method, the contrast between image areas containing cells and background is increased (Figure 3B). This allows accurate object mask placement around cell containing areas (Figure 3C) using the cellular analysis criteria in Table 6.

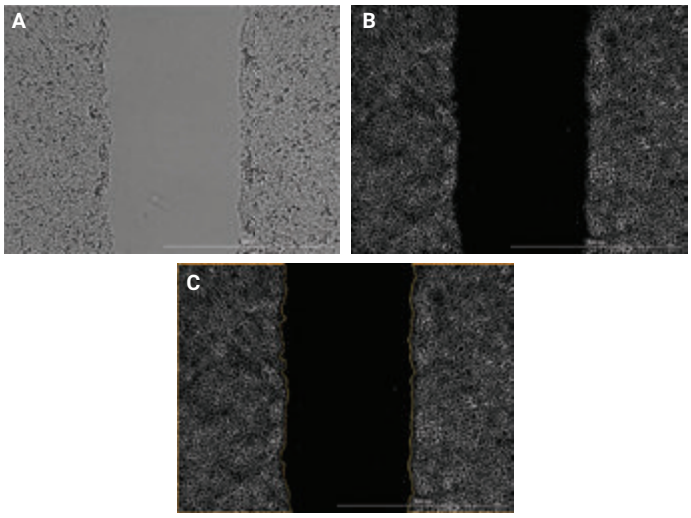

Figure 3. High contrast brightfield image processing and analysis. (A) Raw high contrast brightfield image; (B) preprocessed high contrast brightfield image; and (C) preprocessed high contrast brightfield image with object mask placement.

Using the wound width formula described previously, the average wound width at time 0 following wound creation was generated for each well of the 96- and 24-well plates. The %CV of the wound width values across all wells of the 96-well test plate was calculated to be 2.1%, whereas the %CV of the wound width values across the 24-well test plate was 1.4%, illustrating the high degree of repeatability in created wound size when using the AutoScratch tool with either plate well density.

Cell carryover testing

Because wound creation takes place in a column wise fashion across the microplate, it was necessary to confirm that the cleaning process that follows wounding in each column effectively presents carryover and cross-contamination (cells were not carried from column to column on the pins of the AutoScratch tool). For this experiment, HT-1080 cells in column 1 of a 96-well plate were stained with CellTracker Green fluorescent probe, whereas all other wells in columns 2 to 12 were left unstained (Figure 4).

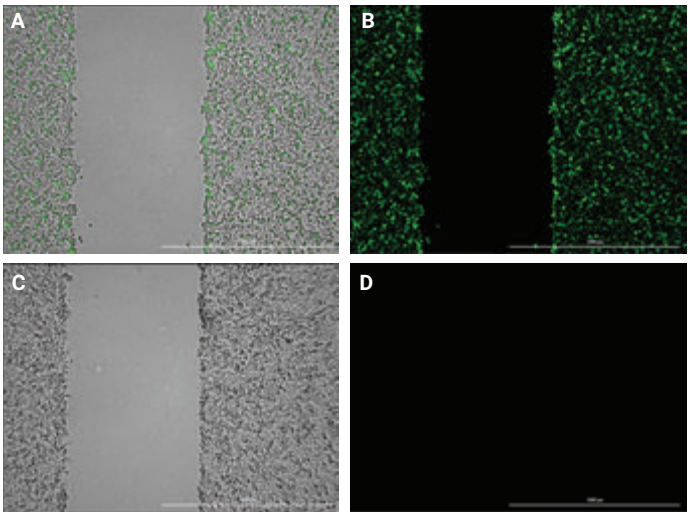

Figure 4. High contrast brightfield and GFP images. (A) High contrast brightfield/GFP overlaid images; and (B) GFP images only following wound creation for CellTracker Green stained cells in column 1. (C) High contrast brightfield/GFP overlaid images; and (D) GFP images only following wound creation for unstained cells in column 2.

Wound creation was then allowed to proceed as previously described. Following image processing, image analysis was performed to quantify the total GFP signal per image. The percent GFP signal in columns 2 to 12 compared to the signal in column 1, per row, was then calculated.

As seen in Figure 5, signal percentages were less than 0.1% for every well subsequent to column 1, demonstrating that the cleaning process following wounding in each column effectively prevents cells from being carried from column to column, eliminating carryover and cross-contamination (carryover and cross-contamination between the columns of each test plate).

Kinetic wound healing metrics

Kinetic imaging of the test plates was then allowed to proceed to monitor cell migration into the wound area. Test plates were added to the BioSpa 8 and robotically transferred to the Cytation 5 at predefined intervals. Due to the fact that HT-1080 cells migrate rapidly, a more frequent imaging interval of 60 minutes was selected to properly capture movement of the cells over time. As with the wound width metric, sum area values were used to calculate wound confluence for each well over the entire incubation period. All metrics for each plate type, including the original sum area values in addition to calculated wound width and wound confluence, were then plotted versus time to assess data consistency by comparing the kinetic curves from each well (Figure 6).

The kinetic sum area graphs were also used to calculate the final kinetic wound healing metric, maximum wound healing rate. From examining the kinetic curves generated from each metric, it is clear that a high degree of similarity is seen from well to well. In addition, the average of the maximum wound healing rate values from each well of the 96- or 24-well plates, at a 95% confidence interval was 1.61 ±0.01 × 10^5 µm^2/hour with a %CV of 3.8% for 96-, and 1.612 ±0.005 × 10^5 µm^2/hour with a %CV of 2.1% for 24-well format, confirm that use of the AutoScratch tool yields kinetic wound healing results with high levels of consistency within wells of a single plate, and also between different plate well formats.

	1	2	3	4	5	6	7	8	9	10	11	12
A		0.02	0.02	0.03	0.02	0.02	0.03	0.02	0.02	0.01	0.02	0.02
B		0.02	0.01	0.03	0.03	0.02	0.05	0.02	0.04	0.02	0.02	0.02
C		0.03	0.03	0.03	0.03	0.02	0.02	0.03	0.02	0.03	0.02	0.03
D		0.03	0.02	0.03	0.03	0.03	0.00	0.03	0.03	0.02	0.02	0.03
E		0.03	0.03	0.03	0.03	0.03	0.10	0.02	0.03	0.03	0.03	0.03
F		0.07	0.07	0.03	0.03	0.03	0.03	0.03	0.03	0.03	0.05	0.03
G		0.03	0.03	0.03	0.03	0.03	0.03	0.03	0.03	0.02	0.03	0.03
H		0.02	0.03	0.02	0.03	0.03	0.05	0.06	0.03	0.05	0.03	0.03

Figure 5. Calculated percent GFP signal carryover values from stained cells in column 1.

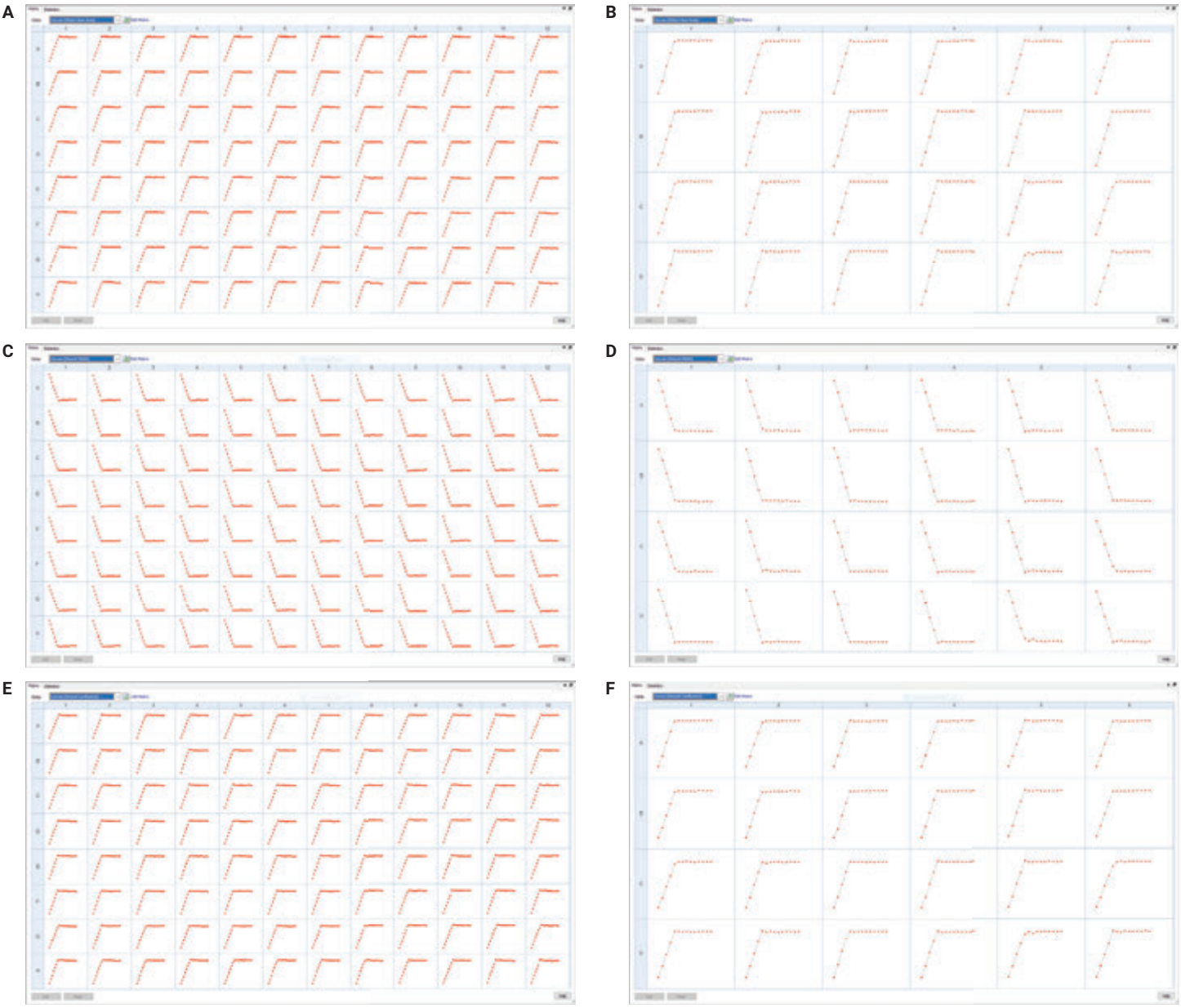

Figure 6. Full plate screenshots of plotted kinetic wound healing metric data. Kinetic sum area, wound width and wound confluence graphs for (A, C, and E) 96- and (B, D, and F) 24-well plates, respectively.

Cell migration inhibition analysis

The AutoScratch tool was also used to prepare for a wound healing inhibition test. Here the automated wounding and washing procedures were carried out as previously described. However, in this case, following the third wash aspiration step, media containing varying concentrations of cytochalasin D was added to the wells. Twelve replicates of an 8-point titration were added across the plate in 96-well format, and four replicates of a 6-point titration were added down the plate in 24-well format. Test plates were once again added to the BioSpa 8 and automatically imaged as previously defined. The kinetic migration curves demonstrate the consistency achieved amongst replicates within each inhibitor concentration (Figure 7).

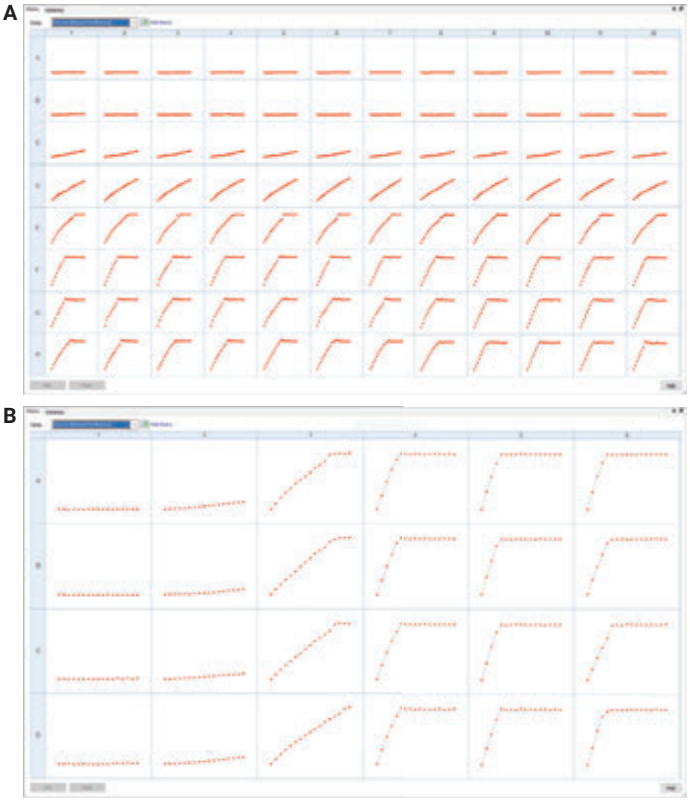

Figure 7. Kinetic cytochalasin D titration wound confluence graphs. (A) 96-well plate containing 12 replicates each of an 8-point titration. Cytochalasin D titrated from 10,000 nM using serial 1:4 dilutions from rows A to G, with row H being no compound negative control. (B) 24-well plate containing 4 replicates each of a 6-point titration. Cytochalasin D titrated from 10,000 nM using serial 1:10 dilutions from column 1 to 5, with column 6 being no compound negative control.

Average kinetic curves from each tested concentration were then plotted on a single graph for data generated in either 96- or 24-well format (Figure 8).

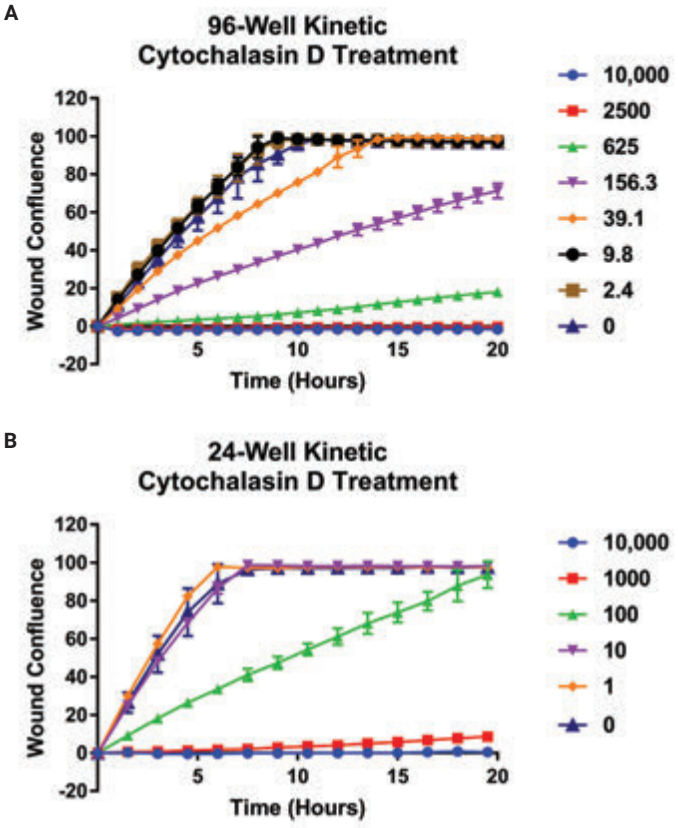

Figure 8. Average kinetic cytochalasin D titration wound confluence graphs. Average, plus/minus standard deviation plotted for each test cytochalasin D concentration at every captured timepoint in (A) 96-well; and (B) 24-well plate formats.

Upon observation of the individual kinetic curves, it is then possible to see the total effect of the compound titration over time. The advantage of being able to collect images over the entire incubation period, and generate kinetic data, as opposed to performing endpoint imaging at a predecided upon time, becomes apparent when comparing IC_{50} curves and values generated from individual incubation periods (Figure 9).

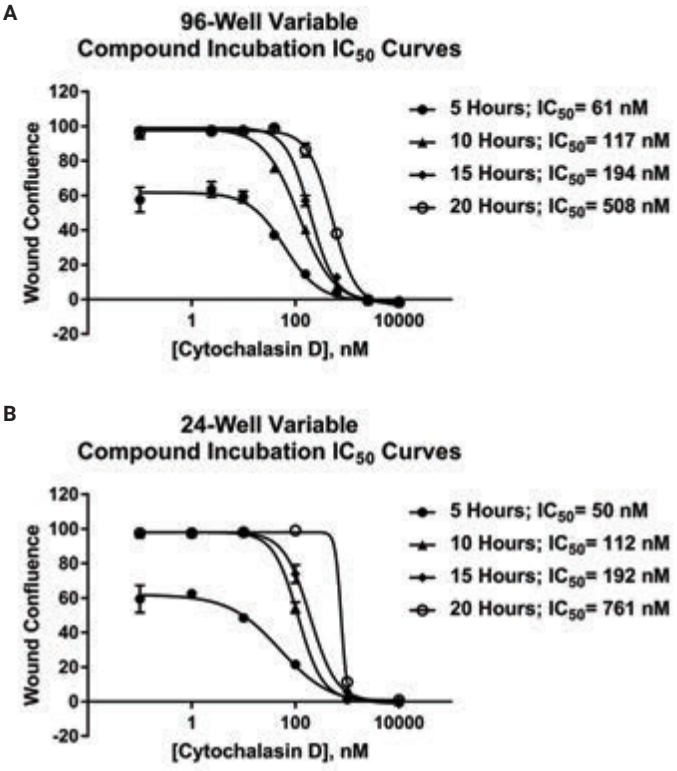

Figure 9. Variable incubation cytochalasin D dose response graphs. Dose response curves and generated IC_{50} values following incubation of HT-1080 cells with cytochalasin D for 5, 10, 15, or 20 hours in (A) 96-well; and (B) 24-well plate formats.

From the 5-hour incubation dose response curves generated from experiments run in either 96- or 24-well format, it is obvious that cell migration is incomplete in negative control and low compound treatment wells. Therefore calculated IC_{50} values would not properly reflect the ability of the compound to inhibit cell migration. By increasing the incubation period by an additional five hours it is then apparent that wells containing little or no compound achieve total wound closure. Complete inhibition is also attained with the highest concentrations, yielding a full dose response and more accurate IC_{50} value. When using a 15-hour incubation period, equivalent dose response curves and IC_{50} values are also seen. However, if the cells are allowed to migrate for 20 hours, dose response curve shapes change dramatically and IC_{50} values increase 2.5 to 3.5x over those seen from the 10- and 15-hour incubation periods. By using the information from the complete data set, a proper incubation period of 10 to 15 hours can then be decided upon for future experiments.

Manual scratch wound creation

Wound creation was also carried out manually using a P200 pipette tip in 96-well format to compare results achieved using a commonly incorporated manual method to those described previously using the AutoScratch tool.

From the images in Figure 10, the variability within each created wound is noticeably greater than those made by the AutoScratch. Images in Figures 10A and 10B show wounds having greater widths at the top of the image, while being visibly smaller towards the bottom of the image. Even when the wound is of a more consistent width down the image (Figure 10C), the lack of verticality can also skew generated results. This is apparent from the %CV calculated using Gen5 generated wound widths from 48 wells where wounds were manually created. The final value of 9.2% is greater than 4x that seen when using the AutoScratch to create wounds in a 96-well plate (2.1%) and greater than 6x that seen when using the AutoScratch to create wounds in a 24-well plate.

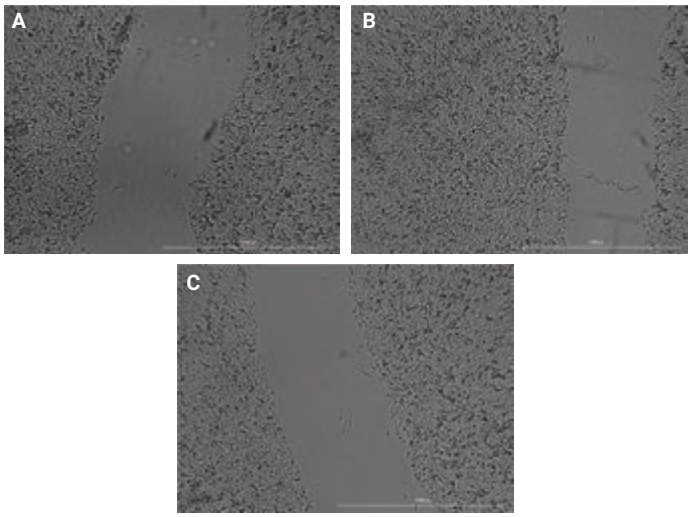

Figure 10. Images captured from a 96-well plate immediately following wound creation with a P200 pipette tip using the high contrast brightfield imaging channel and a 4x objective.

The difference in data quality between plates containing wounds created manually and with the AutoScratch is further illustrated upon view of cytochalasin D dose response curves (Figure 11) generated from kinetic cell migration data.

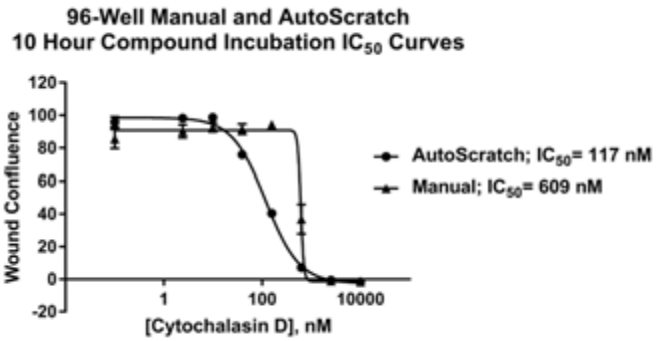

Figure 11. Manual and Agilent BioTek AutoScratch cytochalasin D dose response graphs. Dose response curves and generated IC_{50} values following incubation of HT-1080 cells with cytochalasin D for 10 hours in 96-well plates scratched manually or with the AutoScratch tool.

When using the same compound incubation period, the curve shape lacks the sigmoidal dose response seen with AutoScratch created wounds and the IC_{50} value is 5x greater, which could lead to false assumptions being made regarding the potency of the test molecule when incorporating a manual wounding process.

AutoScratch wound creation using variable size cell models

As a wide variety of cell models are incorporated into 2D scratch wound healing assays, the AutoScratch tool was also used to create wounds using primary fibroblasts and U-87 glioblastoma cells, which have a larger size and different plate attachment pattern compared to HT-1080 cells. Because the Cytation 5 can capture images using both high contrast brightfield and fluorescence, the fibroblasts, which express RFP, and the U-87 cells, which express GFP, could be captured using the high contrast brightfield and either RFP or GFP signal from the cells in a single imaging step (Figure 12).

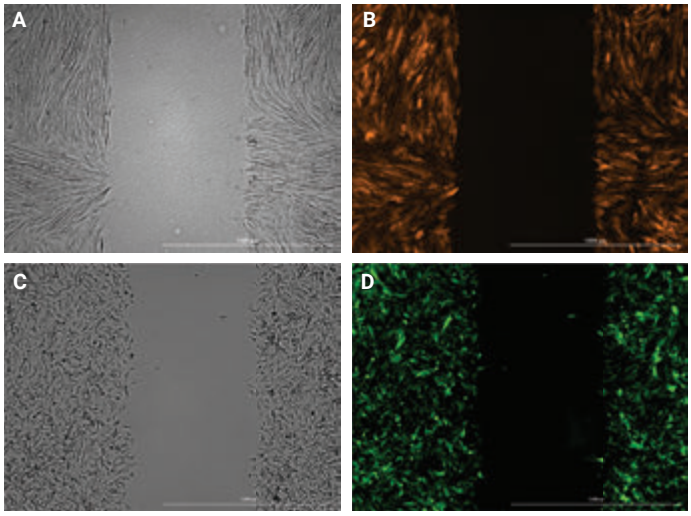

Figure 12. High contrast brightfield and fluorescent images of primary fibroblasts and U-87 glioblastoma cells. (A) High contrast brightfield; and (B) RFP images of RFP expressing primary fibroblasts. (C) High contrast brightfield; and (D) GFP images of GFP expressing U-87 cells.

Percent CV values calculated from wound widths generated at time 0 using high contrast brightfield images across 96 wells for fibroblasts (3.2%), and across 24 wells for U-87 cells (2.6%) demonstrate that the AutoScratch tool can create consistent wounds in each well despite the irregular shape of the cell models.

The similarity in the kinetic wound healing inhibition curves following cytochalasin D treatment of the fibroblasts or U-87 cells (Figure 13), compared to the curves seen in Figure 8 using HT-1080 cells also proves that Gen5 cellular analysis metrics can place accurate object masks around cells of varying size and shape.

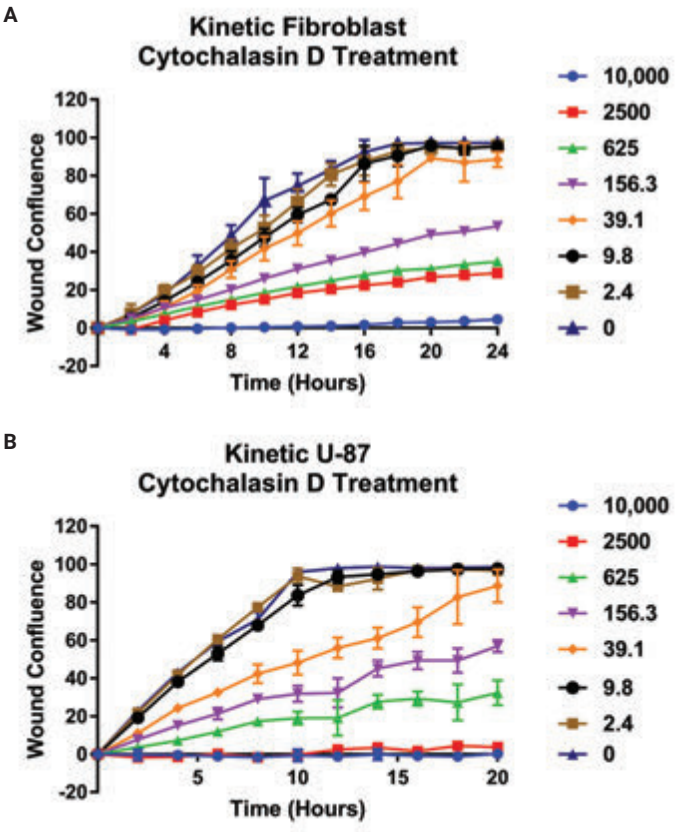

Figure 13. Average fibroblast and U-87 kinetic cytochalasin D titration wound confluence graphs. Average, plus/minus standard deviation plotted for each test cytochalasin D concentration at every captured timepoint with (A) primary fibroblasts; or (B) U-87 cells.

Conclusion

The Agilent BioTek AutoScratch wound making tool creates consistent wounds in an automated fashion in both 96- and 24-well plate formats. The disinfection and sterilization procedure before and after wounding, in addition to cell removal between columns, simplifies cleaning of the tool and also prevents carryover of cells from column to column. When compared to results generated from plates with wounds created manually, initial wound widths and kinetic values show improved reproducibility and increased robustness. The combination of the automated wound creation procedure, kinetic imaging, and Agilent BioTek Gen5 cellular analysis method creates an easy to use, dependable process to carryout wound healing assays.

References

1. Li, L. *et al.* Collective Cell Migration: Implications for Wound Healing and Cancer Invasion. *Burns Trauma*, **2013**, *1(1)*, 21–26.
2. Poujade, M. *et al.* Collective Migration of an Epithelial Monolayer in Response to a Model Wound. *Proc. Natl. Acad. Sci.*, **2007**, *104(41)*, 15988–93.
3. Giampieri, S. *et al.* Localized and Reversible TGFbeta Signalling Switches Breast Cancer Cells from Cohesive to Single Cell Motility. *Nat. Cell Biol.*, **2009**, *11(11)*, 1287–96.
4. Friedl, P.; Hegerfeldt, Y.; Tusch, M. Collective Cell Migration in Morphogenesis and Cancer. *Int. J. Dev. Biol.*, **2004**, *48(5-6)*, 441–9.

www.agilent.com/lifesciences/biotek

RA44216.561724537

Printed in the USA, April 1, 2021
5994-2585EN
AN100118_10

Agilent
Trusted Answers